Development of an Object-Oriented Monte Carlo Simulator for 3D Positron Tomography

H. Zaidi, A. Herrmann Scheurer[*] and C. Morel

Division of Nuclear Medicine, Geneva University Hospital, CH-1211 Geneva 4

1. Introduction

Monte Carlo simulation of 3D PET data is a very powerful tool to check the performance of image reconstruction algorithms and their implementations. Since it allows to obtain separate images of prompt and scattered events, it may help developing and evaluating 3D attenuation and scatter correction techniques. Furthermore, providing its design is easily extendible, it represents an efficient tool to study different 3D PET scanner configurations. We present an object-oriented, extendible design for a Monte Carlo simulator for 3D positron tomography. Preliminary results from phantom simulation studies including attenuation and scattering of the gamma rays in the field-of-view are presented and future prospects discussed.

2. Methods

2.1 Software description

The Monte Carlo simulator, *Eidolon*, was written in Objective-C and runs under NextStep 3.3 on an HP 9000 workstation. A graphical user interface allows one to select scanner parameters such as the number of detector rings, detector material and sizes, discrimination thresholds and energy resolution. It also allows to choose a set of simple 3D shapes, such as parallelepiped, ellipsoid or cylinder, for both the annihilation sources and the scattering media, as well as their respective activity concentrations and chemical compositions. One may view the reference image and the sinograms as they are generated.

2.2 Design

In order to ease the job of incrementally adding capabilities to the Monte Carlo simulator, a modular design featuring dynamically loadable program elements or bundles was adopted. The basic building block is a *model element* class which allows elements to be browsed, inspected, adjusted, created and destroyed through a graphical inspector. This was then used to implement simple parametric source, detector and scatter classes and sinogram and image classes to view and save the generated data in CTI Matrix 6 format. A controller object oversees the simulation process. The reference image and sinogram displays are periodically updated.

The model assumes a cylindrical array of detector crystals and known spatial distributions of annihilation sources and scatter phantoms. Pairs of annihilation photons are generated uniformly within the source objects and are tracked until they expire, either by interacting within scatter or detector objects, or by escaping the PET scanner geometry

---

[*]Present address: Institute of Physiology, University of Lausanne, CH-1015 Lausanne.

and field-of-view. Photoelectric absorption, as well as incoherent and coherent scattering are taken into account to simulate photon interaction within scatter and detector objects. Interaction cross-sections and scattering distributions are computed from parametrizations that were implemented in the GEANT simulation package of CERN. Interaction within scatter or detector objects can be switched on and off interactively. In case interaction within detector objects is switched off, any photon impinging on a detector is assumed to deposit all its energy in the detector crystal. Energy resolution of the detector is simulated by convolving the deposited energy with a Gaussian function. Photon pairs are recorded in the sinogram object once two photons resulting from one annihilation event have passed the energy window set for discrimination.

3. Results

The time needed to perform a simulation study depends on the complexity of the chosen sets of source, scatter and detector objects, and on selected interactions. The average time to track one coincident detection for the ECAT-953B PET scanner (16 detector rings, 256 sinograms, 96 views of 128 elements each) is 1.15 ms without scattering nor attenuation. It increases to 11 ms if photon interaction is simulated within a single uniform scatter object corresponding to a 20 cm diameter cylinder filled with water, and to 15.2 ms if it is simulated within both the scatter and the detector objects.

Eidolon was used to obtain unscattered and scattered energy distributions of coincident detections (*Fig. 1*), as well as to study line-spread functions (*Fig. 2*) and scatter fractions for the ECAT-953B PET scanner. The scatter fraction is defined as the ratio between the number of coincident detections with at least one photon scattered in the field-of-view and the total number of coincident detections. *Table 2* shows scatter fractions obtained with *Eidolon* for three different radial positions of a line source placed in a 20 cm diameter cylinder filled with water. Ten million annihilation events were generated for each radial position of the line source. The scatter fraction determined with the line source in the centre of the phantom is 0.37. In the same detection conditions, a real measurement of this scatter fraction gave 0.42 [1] and it was estimated to be 0.46 using a different Monte Carlo simulator [2]. The discrepancy between our value and the one given in Ref. 2 results from the fact that photons which are scattered only within the detector crystals are not considered to be scattered regarding the scatter fraction determination, as they are in Ref. 2. As for real measurements, the scatter fraction decreases when the source moves off-axis.
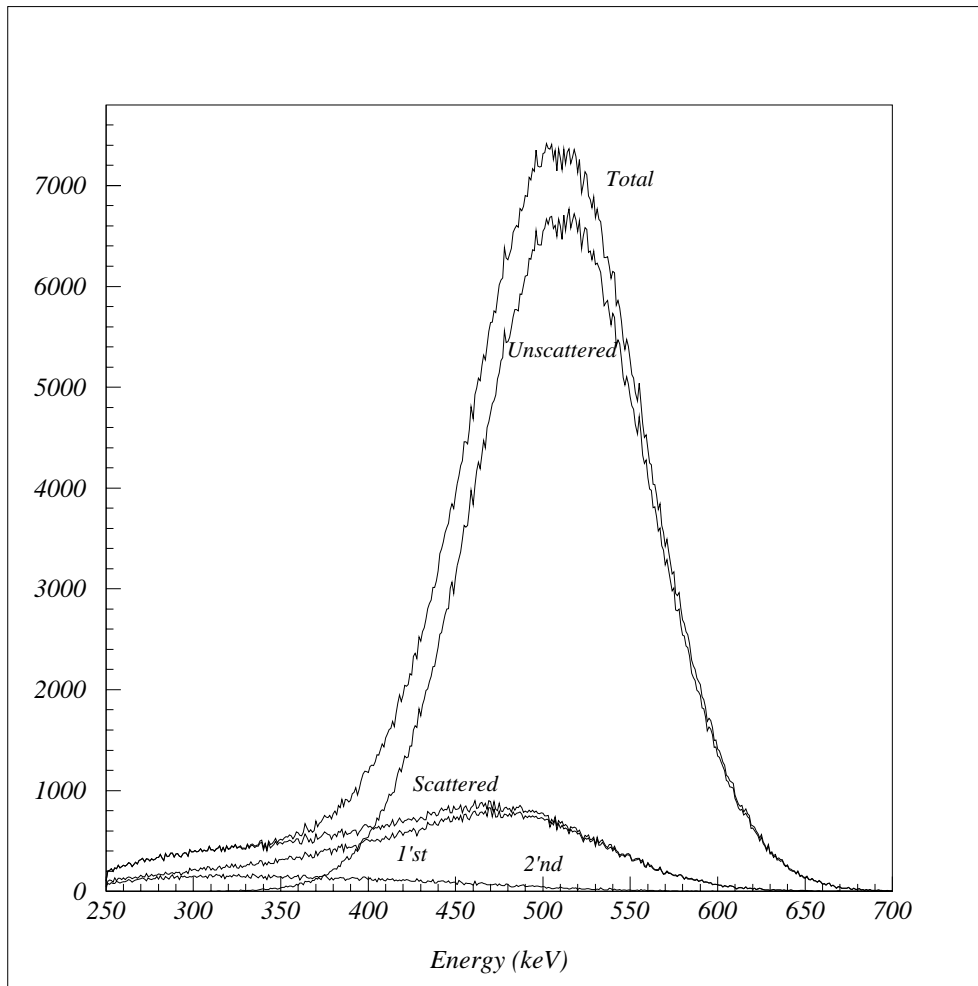
Figure 1: Energy distributions of coincident detections resulting from the simulation of a line source placed in the centre of a 20 cm diameter cylinder filled with water. Photons impinging on a detector are assumed to deposit all their energy in the detector crystal. Energy resolution is proportional to the inverse square root of the deposited energy and is simulated by convolving the deposited energy with a Gaussian function whose FWHM is 23% for 511 keV photons. Both photons of a coincident detection have to pass an energy window set between 250 and 850 keV. Distributions of photons resulting from exactly one or two successive Compton scatterings in the field-of-view are shown.

| Radial position [mm]	*Eidolon*	Spinks [1]	Michel [2]
0	0.37	0.42	0.46
40	0.36	0.40	
80	0.29	0.30	

Table 1: Comparison between Monte Carlo estimations and real measurements of the scatter fraction for different radial positions of a line source placed in a 20 cm diameter cylinder filled with water. Same detection conditions as in *Figure 1* apply, except that interaction within detector objects was switched on and energy window was set between 380 and 850 keV for comparison with Ref. 1.

Eidolon was also used to simulate the Utah phantom which is designed with a high degree of inhomogeneity both transaxially and axially in order to compare and test scatter correction techniques in 3D PET. Utah phantom data sets for the ECAT-953B PET scanner were generated both with and without scatter simulation (*Fig. 3*). The outer compartment of the phantom which is generally used to provide activity from outside the field-of-view is kept empty. Generated data sets were reconstructed using four different exact and approximate 3D reconstruction algorithms implemented of a high performance parallel platform [3]. Attenuation corrections were applied before reconstruction to the data sets generated with scatter simulation. The attenuation correction files were created by forward projecting the 3D density map estimated with a constant linear attenuation coefficient of 0.096 cm^{-1}.

4. Discussion and conclusion

Validation of image reconstruction implementations and scatter correction techniques, as well as design of new 3D PET systems using the Monte Carlo method have received considerable attention during the last decade and a large number of applications have been developed. The object-oriented paradigm makes it possible to envision incremental refinements to any of the elements described in this extended abstract with maximum code reuse by providing a framework for effectively defining standards using the inheritance mechanism. This approach streamlines development and improves reliability. It makes *Eidolon* a very powerful tool that can be further modified to
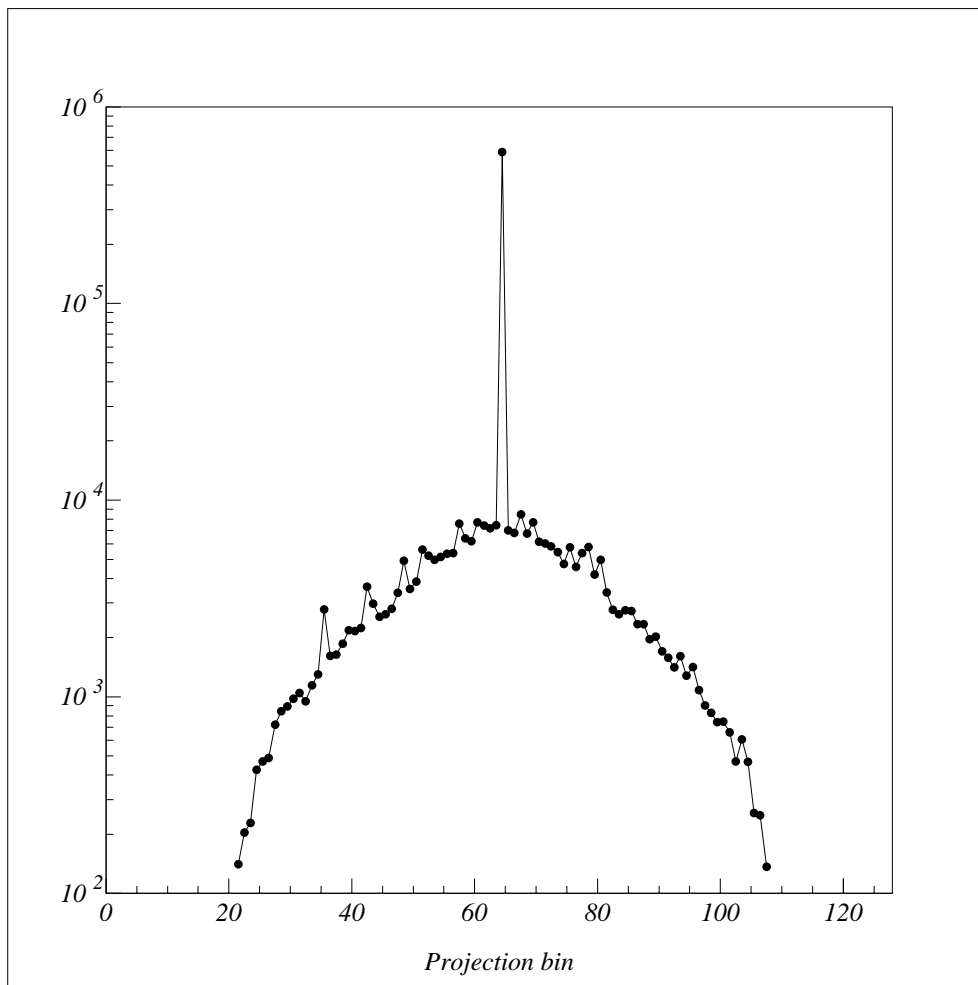
Figure 2: Sum of one-dimensional transaxial projections resulting from the simulation of a line source placed in a 20 cm diameter cylinder filled with water. Same detection conditions as in *Figure 1* apply.

investigate new possible designs of high performance positron tomographs. Eventually, *Eidolon* will be exploited to explore different sampling schemes of the 3D X-Ray transform.

Although variance reduction techniques have been developed to reduce the computation time, the main drawback of the Monte Carlo method is that it is extremely time-consuming. With the development of parallel-processing computers, researchers have turned their efforts towards the parallelisation of Monte Carlo codes. An implementation of *Eidolon* on a parallel system with 8 PowerPC-604 nodes that was recently installed in our laboratory is being presently undertaken.

References

[1] T.J. Spinks, T. Jones, D.L. Bailey, *et al.*, "Physical performance of a positron tomograph for brain imaging with retractable septa", *Phys. Med. Biol.* **37** (1992) 1637-1655.

[2] C. Michel, A. Bol, T. Spinks, D. Townsend, D. Bailey, S. Grootoonk and T. Jones, "Assessment of response function in two PET scanners with and without interplane septa", *IEEE Trans. Med. Imag.* **10** (1991) 240-248.

[3] M.L. Egger, A.K. Herrmann Scheurer, C. Joseph and C. Morel, "Fast volume reconstruction in positron emission tomography: Implementation of four algorithms on a high-performance scalable parallel platform", to appear in *Conf. Rec. 1996 IEEE Med. Imag. Conf.*, Anaheim, CA, 1996.

[4] P.E. Kinahan and J.G. Rogers, "Analytic 3D image reconstruction using all detected events", *IEEE Trans. Nucl. Sci.* **36** (1989) 964-968.

[5] M. Defrise, D.W. Townsend and R. Clack, "Favor: a fast reconstruction algorithm for volume imaging in PET", in *Conf. Rec. 1991 Med. Imag. Conf.*, Santa Fe, NM, 1991, pp. 1919-1923.

[6] M. Defrise, "A factorization method for the 3D X-Ray transform", *Inverse Problems* **11** (1995) 883-994.

[7] M.E. Daube-Witherspoon and G. Muehllehner, "Treatment of axial data in three-dimensional PET", *J. Nucl. Med.* **82** (1987) 1717-1724.
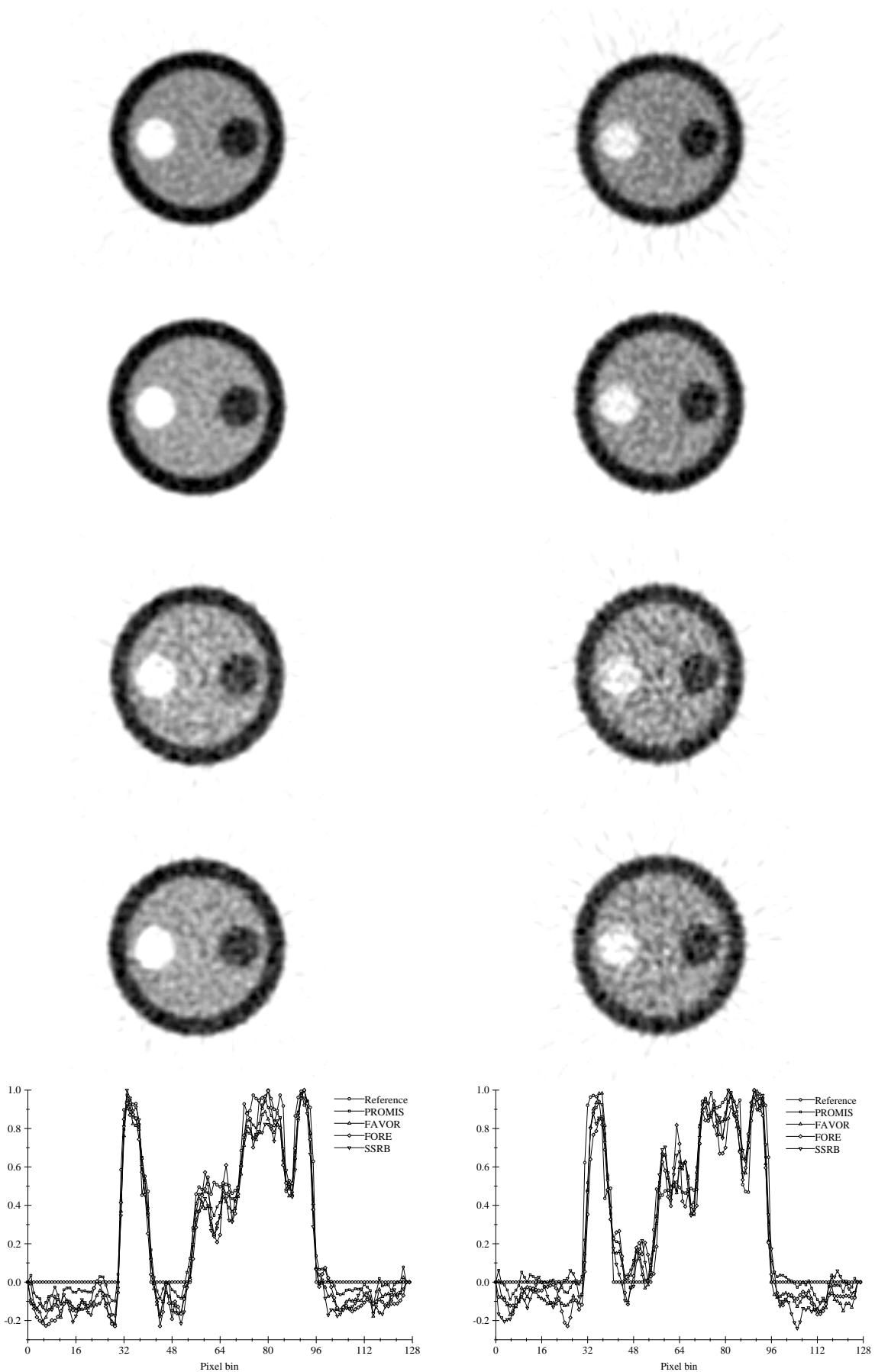
Figure 3: Eleventh slice reconstructions of Monte Carlo data sets of the Utah phantom generated without (left) and with (right) scatter simulation. The reconstruction algorithms used are (from top to bottom): the Kinahan and Rogers reprojection algorithm [4], the Fast Volume Reconstruction algorithm (FAVOR) [5], the Fourier Rebinning algorithm (FORE) [6] and the Single-Slice Rebinning algorithm (SSRB) [7]. Same detection conditions as in *Figure 1* apply. Seven million coincident detections were recorded for both types of simulations. The maximum obliquity used for reconstruction corresponds to a ring index difference of 11. No additional polar or azimuthal mashing was used. Horizontal profiles through the centre of the slices are also shown.